Published OnlineFirst September 9, 2014; DOI: 10.1158/1535-7163.MCT-14-0599

Large Molecule Therapeutics

Molecular Cancer Therapeutics

A Chemically Defined Trifunctional Antibody–Cytokine–Drug Conjugate with Potent Antitumor Activity

Thomas List[1], Giulio Casi[2], and Dario Neri[1]

Abstract

The combination of immunostimulatory agents with cytotoxic drugs is emerging as a promising approach for potentially curative tumor therapy, but advances in this field are hindered by the requirement of testing individual combination partners as single agents in dedicated clinical studies, often with suboptimal efficacy. Here, we describe for the first time a novel multipayload class of targeted drugs, the immunocytokine–drug conjugates (IDC), which combine a tumor-homing antibody, a cytotoxic drug, and a proinflammatory cytokine in the same molecular entity. In particular, the IL2 cytokine and the disulfide-linked maytansinoid DM1 microtubular inhibitor could be coupled to the F8 antibody, directed against the alternatively spliced EDA domain of fibronectin, in a site-specific manner, yielding a chemically defined product with selective tumor-homing performance and potent anticancer activity *in vivo*, as tested in two different immunocompetent mouse models. *Mol Cancer Ther; 13(11); 2641–52. ©2014 AACR.*

Introduction

Modern pharmacotherapy of cancer increasingly makes use of drug combinations, which may display a synergistic therapeutic activity *in vivo*, acting through complementary mechanisms of action (1–5). In practice, however, the combination of pharmaceutical agents is difficult to implement in the clinic, as the individual drugs typically need to be extensively studied as single agents, before they can be considered for combination trials. This procedure is expensive, time-consuming, and may deny patients a timely access to pharmacologically active treatments.

Cytotoxic agents remain the backbone of cancer pharmacotherapy. In many cases, cytotoxic drugs represent ideal combination partners for immunostimulatory agents (e.g., checkpoint-inhibitory antibodies, cytokines), as the 2 classes of compounds exhibit different and mutually compatible toxicity profiles, while exploiting complementary mechanisms of action. In preclinical studies, the therapeutic activity of IL2-based immunocytokines was strongly potentiated by the combination with the mitotic inhibitor paclitaxel (2, 6), doxorubicin (6), temozolomide (7), and with sunitinib (8). In addition, tumor-targeting immunocytokines are being studied in clinical trials in combination with dacarbazine (9), gemcitabine (9–11), melphalan (12), fenretinide (13), doxorubicin (6), and paclitaxel (14, 15).

Emerging experimental evidence indicates that cytotoxic drugs may act on the tumor endothelium and favor the extravasation of therapeutic agents while also promoting the expression of stress proteins on cancer cells, which can be recognized by leukocytes *in vivo*. For example, increased vascular permeability (2), reduction of interstitial fluid pressure (16, 17), increased infiltration, and local activation of leukocytes (2, 18) have been proposed as key determinants for the antitumor activity of paclitaxel, one of the most broadly used anticancer drugs with microtubular-inhibitory activity.

The therapeutic index of both cytotoxic drugs and cytokines can be strongly enhanced when these potent payloads are coupled to tumor-homing antibodies, serving as selective pharmacodelivery agents (10). Antibody–drug conjugates (ADC) are armed versions of monoclonal antibodies, which may deliver a highly potent cytotoxic agent at the tumor site, thus helping spare normal tissues (19, 20). Similarly, a large number of proinflammatory cytokines have been genetically fused to tumor-targeting recombinant antibodies, yielding fusion proteins (termed "immunocytokines") which display a potent therapeutic activity in mouse models of the disease and encouraging results in patients with cancer (6, 7, 9, 11, 14, 15, 21–27).

For many applications, antibodies specific to splice isoforms of extracellular matrix components may represent ideal vehicles for the delivery of both cytotoxic drugs and cytokines (28–32). For example, the alternatively spliced EDA domain of fibronectin is virtually undetectable in normal adult tissues (exception made for placenta, for the endometrium in the proliferative phase, and for

[1]Department of Chemistry and Applied Biosciences, Swiss Federal Institute of Technology (ETH Zürich), Zurich, Switzerland. [2]Philochem AG, Otelfingen, Switzerland.

Note: Supplementary data for this article are available at Molecular Cancer Therapeutics Online (http://mct.aacrjournals.org/).

Corresponding Author: Dario Neri, Department of Chemistry and Applied Biosciences, Swiss Federal Institute of Technology (ETH Zürich), Vladimir-Prelog-Weg 4, HCI, CH-8093 Zurich, Switzerland. Phone: 41-44-6337401; Fax: 41-44-6331358; E-mail: dario.neri@pharma.ethz.ch

doi: 10.1158/1535-7163.MCT-14-0599

Published OnlineFirst September 9, 2014; DOI: 10.1158/1535-7163.MCT-14-0599

some vessels in the ovaries; ref. 33) but is strongly expressed around neovascular structures and in the interstitium of most aggressive solid tumors (34), lymphomas (35), and acute leukemias (36). In particular, the F8 monoclonal antibody recognizes the human and murine EDA domain of fibronectin with identical affinity, thus facilitating the study of antibody derivatives both in syngeneic immunocompetent mouse models of cancer and in human tumors. The F8 antibody selectively localizes to tumor blood vessels *in vivo*, as revealed by quantitative biodistribution studies with radioiodinated protein preparations and by *ex vivo* microautoradiographic analysis (37). The antibody retains its tumor-homing properties when used in various formats (e.g., diabody, small immune protein, and IgG), with a residence time of several days in the tumor extracellular matrix (33).

IL2 is a proinflammatory cytokine that induces the activation and proliferation of T cells and natural killer (NK) cells *in vivo*. Recombinant human IL2 is a marketed anticancer product, which can cure patients with metastatic melanoma or with kidney cancer (3, 38–40), albeit at the expense of severe toxicities. Several antibody–IL2 fusion proteins have been tested in mouse models of cancer, and some have progressed to clinical trials in patients with solid malignancies (9, 41) or acute leukemias (36). The F8–IL2 fusion protein has previously exhibited a potent antitumor activity in various mouse models of cancer (2, 8, 36, 42), which can be potentiated by the addition of other therapeutic agents. Importantly, the F8 antibody has also been shown to act as a convenient pharmacodelivery agent for highly potent cytotoxic drugs (e.g., the DM1 maytansinoid, a microtubular inhibitor), when equipped with a suitable linker for cleavage at the site of disease (43). A combination of F8–IL2 with F8-based antibody–drug conjugates mediated a potent anticancer activity, leading to complete eradication of C1498 tumors in immunocompetent mice. The process was found to be dependent both on the action of $CD8^+$ T cells and of NK cells, as revealed by antibody-based immunodepletion studies (27).

In this article, we describe a novel class of trifunctional armed antibody products (termed "immunocytokine drug conjugate," or IDC), which can be efficiently prepared with high biochemical purity and with full retention of functional activity of the 3 moieties present in the molecule (i.e., antigen binding, cytokine activity, and drug-mediated cytotoxic activity upon linker cleavage). In particular, the F8–IL2–SS–DM1 IDC product, featuring the simultaneous presence of IL2 and disulfide-linked DM1 drug on a recombinant F8 antibody scaffold in diabody format, selectively localized to solid tumors after intravenous administration and mediated a potent anticancer activity in 2 immunocompetent mouse models (F9 and C1498).

Materials and Methods

Construction of immunocytokine

The F8–IL2–SH and F8–IL2 immunocytokines were genetically assembled by successive PCR assembly steps, in analogy to previously published procedures (8) and cloned into pcDNA3.1 expression vector (Invitrogen) downstream of a mammalian secretion signal sequence. In the case of F8–IL2–SH, one extra amino acid (cysteine) was introduced into the 21 aa linker, yielding a 22 aa linker to obtain one free thiol group on the cysteine side chain for site-specific drug coupling reactions. The complete gene sequences for the F8–IL2–SH, F8–IL2, and F8–SH products can be found in the Supplementary Data.

Cell lines and mice

Chinese Hamster Ovary cells (CHO-S, obtained from Invitrogen, 2007) cells were used for the production of recombinant proteins. The tumor cell lines used for cytotoxicity assays and therapy studies were the murine teratocarcinoma cell line F9 (CRL-1720, obtained from ATCC, 2003), the murine acute myelogenous leukemia (AML) cell line C1498 (TIB-49, obtained from ATCC, 2008), the murine B-cell lymphoma cell line A20 (TIB-208, obtained from ATCC, 2008), and the murine melanoma cell line K1735M2 which was a kind gift of Prof. Silvio Hemmi (University of Zürich, Zürich, Switzerland). For T-cell activation experiments, the murine cytotoxic T-cell line CTLL2 was used (TIB-214, obtained from ATCC, 2004). CHO-S cells in suspension were cultured in shaker incubators (37°C) in PowerCHO-2CD medium (Lonza) containing 8 mmol/L ultraglutamine (Lonza) and HT supplement (Lonza). F9 cells were cultured on 0.1% gelatin-coated tissue flasks or wells in DMEM (Thermo Scientific) supplemented with 10% FCS (Thermo Scientific) and antibiotic–antimycotic (Thermo Scientific) at 37°C and 5% CO_2. C1498 cells were cultured in DMEM supplemented with 10% FCS, 1 mmol/L sodium pyruvate (Thermo Scientific) at 37°C and 5% CO_2. A20 cells were cultured in RPMI-1640 (Thermo Scientific) with 10% FCS, 0.05 mmol/L β-mercaptoethanol (Thermo Scientific), and antibiotic–antimycotic at 37°C and 5% CO_2. K1735 cells were cultured in DMEM with 10% FCS, 1 mmol/L sodium pyruvate (Thermo Scientific), and antibiotic–antimycotic at 37°C and 5% CO_2. CTLL2 cells were cultured at 37°C and 5% CO_2 in RPMI-1640 medium (Thermo Scientific) supplemented with 10% FCS, antibiotic–antimycotic, 1 mmol/L sodium pyruvate, 50 μmol/L β-mercaptoethanol, human IL2 (20 units/mL; Sino Biological), and 1% v/v ultraglutamine. Female 129/SvFv mice and female C57BL/6J mice were obtained from Charles River. Cell lines were obtained from Invitrogen or ATCC cell bank and passaged in our laboratory according to the recommended protocols. No further authentication was performed.

Protein expression and purification

Immunocytokines were expressed using transient gene expression procedures (44). For 200 mL of production, 200×10^6 CHO-S cells were resuspended in 100 mL $ProCHO_4$ (Lonza). Plasmid DNA (250 μg) was mixed with 150 mmol/L NaCl to reach a final volume of 5 mL. Five

Published OnlineFirst September 9, 2014; DOI: 10.1158/1535-7163.MCT-14-0599

milliliters of 250 mg/mL 25-kDa linear polyethylene imine (PEI; 1 mg/mL solution in water at pH 7.0; Polysciences) in 150 mmol/L NaCl was added to the DNA/NaCl solution and allowed to stand at room temperature for 10 minutes. The solution containing the PEI–DNA complexes was then added to the cells and gently mixed. The transfected cultures were incubated in a shaker incubator at 37°C. At 4 hours after transfection, the culture was diluted with 100 mL Power-CHO-2CD medium and then incubated at 31°C in a shaking incubator for 6 days. The fusion proteins were purified from the cell culture medium by protein A affinity chromatography and then dialyzed against PBS (6 mg/mL NaCl, 3.12 mg/mL NaH_2PO_4, 5.34 mg/mL Na_2HPO_4, 300 mmol/L NaOH, pH 7.4).

Conjugation of protein to small molecules

Conjugation of fusion proteins to small-molecule drug (DM1) was performed as previously described by our group (45). Briefly, the proteins in saline solution were reduced under mild conditions with 30 molar equivalents tris(2-carboxyethyl)phosphine (TCEP) 3 hours at room temperature. Free thiol groups were reacted 40 minutes at room temperature with 1,000 molar equivalents 5,5′-dithiobis-(2-nitrobenzoic acid) (DTNB) added to the reduced protein solution. Excess DNTB, which was not covalently bound to protein, was removed by buffer exchange column (PD-10, GE Healthcare) according to manufacturer's protocol for microgram scale production or by HiTrap (GE Healthcare) columns using an FPLC

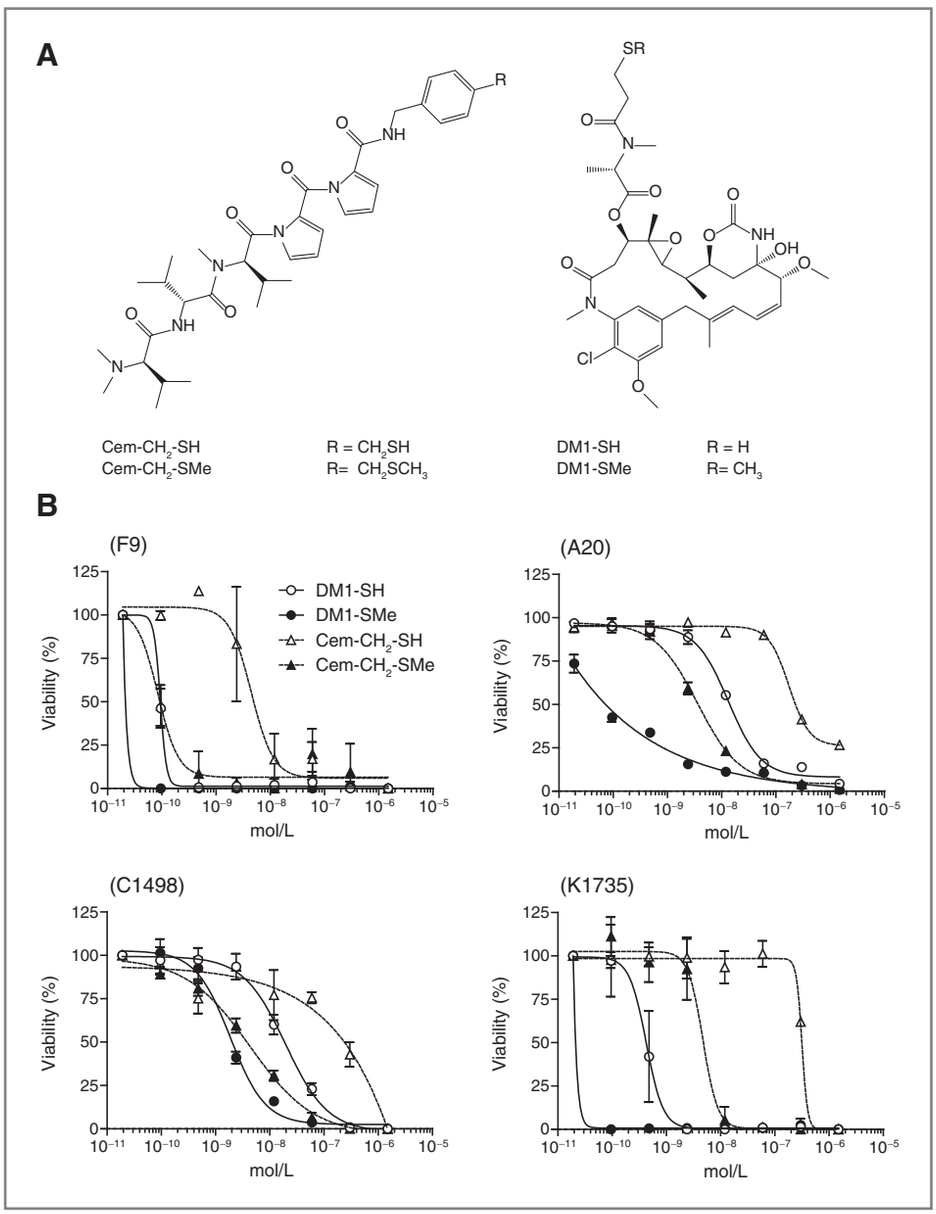

Figure 1. The F9 and C1498 murine tumor cell lines are more susceptible to DM1 than cemadotin. A, cemadotin and DM1 cytotoxic drug and derivatives containing either a free thiol (Cem-CH_2-SH, DM1-SH) or an alkyl group (Cem-CH_2-Me, DM1-SMe). B, dose-dependent percent viability (72-hour endpoint measurement) of 4 murine cell lines *in vitro* with different concentrations of DM1-SH (open circle), DM1-SMe (filled circle), Cem-CH_2-SH (open triangle), and Cem-CH_2-SMe (filled triangle) as measured my MTS colorimetric assay. Viability is given as a percentage of the absorption signal (490 nm) of control cells incubated with culture medium alone.

Published OnlineFirst September 9, 2014; DOI: 10.1158/1535-7163.MCT-14-0599

pump (Äkta Purifier, GE) for milligram scale production. The coupling buffer was 150 mmol/L PBS, pH 7.4, containing 5% w/v sucrose and 10% *N*,*N*-dimethylacetamide (DMA; Acros Organics). Subsequently, protein–DTNB conjugates were reacted with 15 molar equivalents DM1-SH for 5 minutes at room temperature, and the

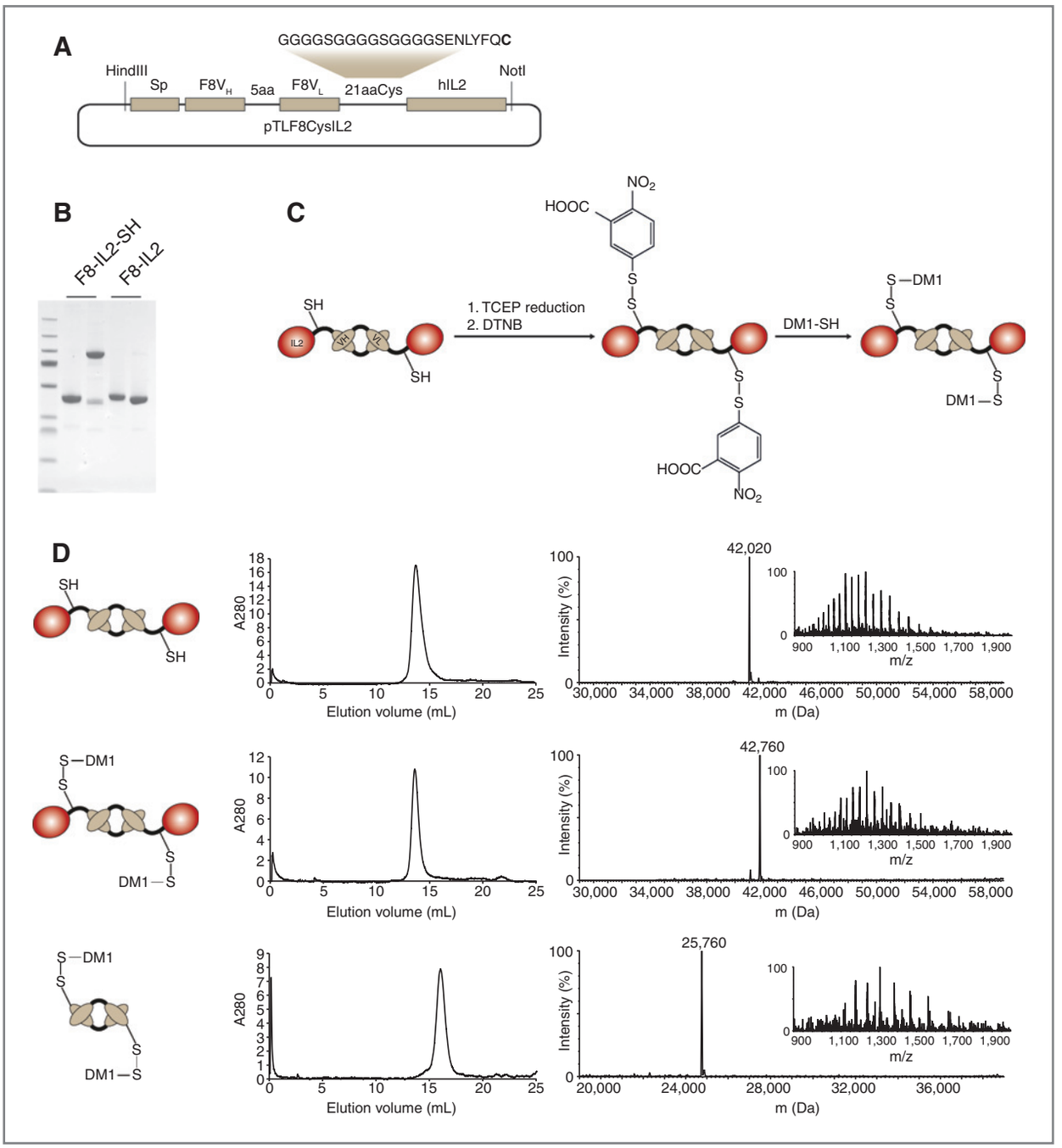

Figure 2. Biochemical characterization of the F8–IL2–SS–DM1 IDC. A, genetic construct for F8–IL2–SH. Sp, posttranslationally cleaved excretion signal peptide; F8V$_H$, variable domain heavy chain; F8V$_L$, variable domain light chain; 5aa, short 5 amino acid linker; 21aaCys, long 22 amino acid linker containing cysteine; hIL2, human IL2. B, PAGE analysis of F8–IL2–SH and F8–IL2 expressed in CHO cells and purified by Protein A affinity chromatography. Reducing conditions with β-mercaptoethanol (lanes 1 and 3) and nonreducing conditions (lanes 2 and 4). C, conjugation of proteins containing a free cysteine to DM1-SH. Protein is reduced with TCEP, activated with DTNP (Ellmann reagent), and conjugated to DM1-SH by disulfide bridge formation. D, profiling of F8–IL2–SH, F8–IL2–SS–DM1, and F8–SS–DM1 by gel filtration (GE S200 10/300GL, Äkta Pure) and MS (ESI, Quadrupole). Elution profiles show the expected retention volumes and MS shows the expected masses of unconjugated and conjugated proteins: 42,016.6 Da (calculated) and 42,020 Da (measured) for the F8–IL2–SH monomer; 42,754.9 Da (calculated) and 42,760 Da (measured) for the F8–IL2–SS–DM1 monomer.

Published OnlineFirst September 9, 2014; DOI: 10.1158/1535-7163.MCT-14-0599

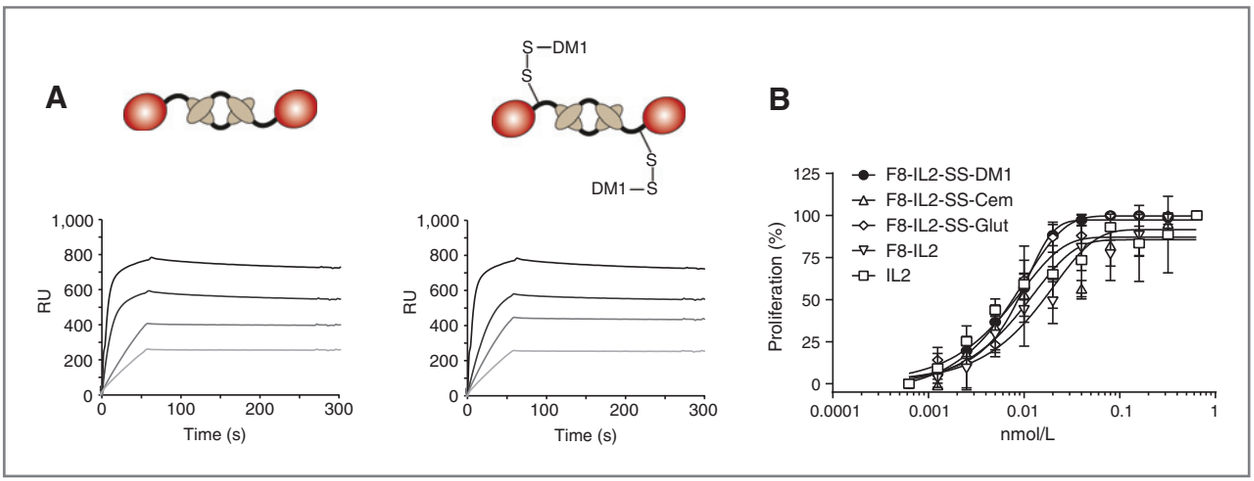

Figure 3. F8–IL2–SS–DM1 is biologically active *in vitro*. A, surface plasmon resonance (Biacore) analysis of difference concentrations of F8–IL2, F8–IL2–SS–DM1, and F8–SS–DM1 on a CM5 chip coated with soluble EDA antigen. B, T-cell stimulatory properties of the IL2 moiety of ADC was benchmarked against commercially available IL2. Dose-dependent percent proliferation (48-hour endpoint) of the CTLL2 murine cell line *in vitro* with different concentrations of F8 conjugates was measured by MTS colorimetry. Proliferation is given as a percentage of the absorption signal (490 nm) of control cells incubated with culture medium alone. F8–IL2–SS–DM1, DM1 conjugate; F8–IL2–SS–Cem, cemadotin conjugate; F8–IL2–SS–Glut, glutathione conjugate.

reaction was quenched with 500 molar equivalents iodoacetamide for 10 minutes at room temperature. Excess DM1 and iodoacetamide were removed in analogy to the procedure described for protein–DTNB conjugates. Characterization of conjugate was performed on an ÄKTA Pure FPLC system with Superdex200 10/300 GL column (size exclusion) and mass spectrometry (MS; ESI-Quadrupole).

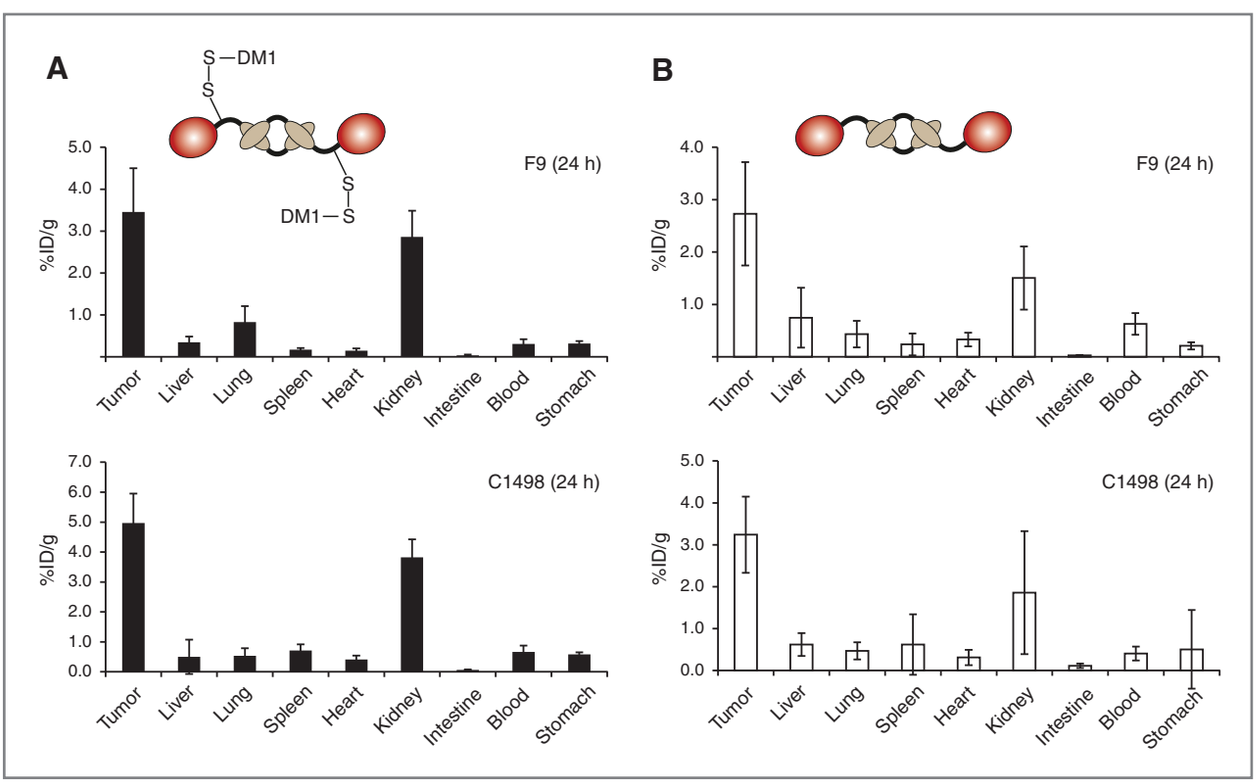

Figure 4. F8–IL2–SS–DM1 selectively accumulates at the tumor site. Immunocompetent mice bearing F9 or C1498 syngeneic tumors were injected with 10 μg (0.09 nmol) 125I radiolabeled (A) F8–IL2–SS–DM1 or (B) F8–IL2. Bars show the mean ± SD percentage injected dose per gram of tissue (%ID/g). Immunoreactivity after radioiodination was confirmed by binding to EDA resin (data not shown).

Published OnlineFirst September 9, 2014; DOI: 10.1158/1535-7163.MCT-14-0599

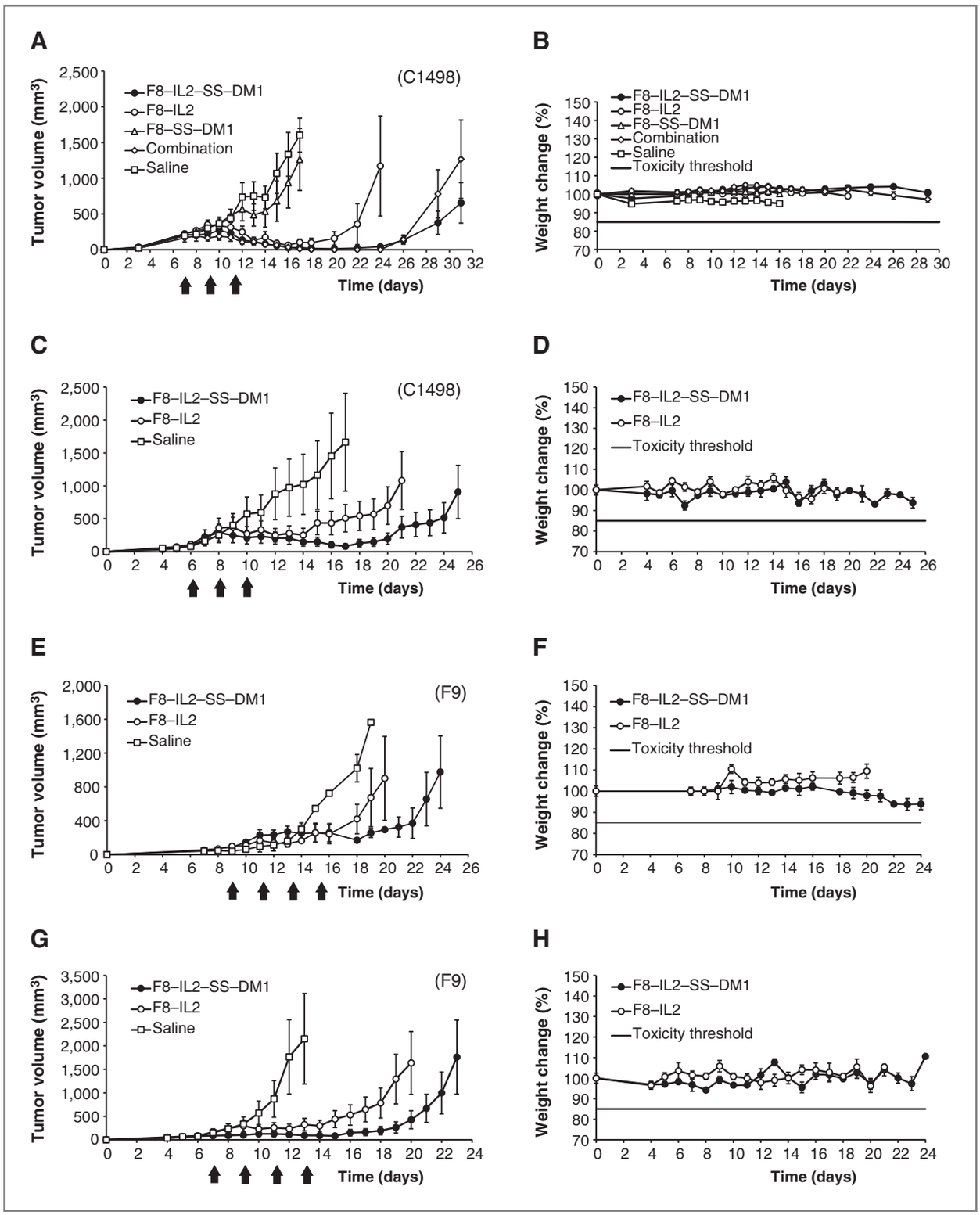

Figure 5. F8–IL2–SS–DM1 matches the antitumor effect of combination therapy and shows improved tumor retardation over the single-payload immunocytokine F8–IL2. Therapy experiments were performed twice for each tumor model with increasing dosage. A, mean tumor volume ± SD (mm^3) is shown over time in 129Sv mice ($n = 4$ per treatment group) implanted s.c. with F9 tumor cells. Mice were injected i.v. in the tail vein with 10 μg conjugate, immunocytokine, or saline every 48 hours for 3 injections in total (arrows). (*Continued on the following page*.)

Published OnlineFirst September 9, 2014; DOI: 10.1158/1535-7163.MCT-14-0599

Surface plasmon resonance

Protein solutions were filtered [using 0.22-μm polyvinylidene difluoride (PVDF) filters] and their binding properties analyzed using a BIAcore3000 instrument (BIAcore) and an antigen coated chip, which was prepared by covalent coupling of bacterially produced EDA to a CM5 sensor chip (GE Healthcare) according to the manufacturer's protocol.

Cytotoxicity assay

Tumor cell lines were seeded at different densities in 96-well plates to achieve a starting confluency of approximately 10% to 20%. The optimal seeding cell densities for different cell types were determined by light microscopic monitoring of confluence and growth rate as follows: 10,000 cells per well for A20, 8,000 cells per well for C1498, 6,000 cells per well for F9, and 10,000 cells per well for K1735. All cell types were grown for 1 week before the experiment to ensure stable growth and seeded in triplicates in 96-well plates at 37°C, 5% CO_2. After 24 hours, different dilutions of drugs in culture medium containing 0.3% DMSO were added to the cells and cultures were incubated for 72 hours at 37°C, 5% CO_2. After 72 hours, 20 μL MTS solution (CellTiter96 AQueous One Solution) was added to each well, cultures were incubated at 37°C, 5% CO_2 for 24 hours, and absorption at 490 nm of each well was measured on a Molecular Devices SpectraMax Paradigm spectrophotometer.

Cell proliferation assay

CTLL2 cells were grown for 2 weeks in fully supplemented growth medium with a maximum density of 10^5 cells/mL. Cells were then starved of IL2 by washing away old growth medium and culturing them in medium lacking IL2 for 48 hours. Starved cells were seeded in 96-well plates at 2×10^4 cells per well and incubated with different dilutions of antibody–drug conjugate or unconjugated IL2 (Proleukin, Aldesleukin, Novartis) for 24 hours at 37°C, 5% CO_2. After 24 hours, 20 μL MTS solution (CellTiter96 AQueous One Solution, Promega) was added to each well, cultures were incubated at 37°C 5% CO_2 for 24 hours, and absorption at 490 nm of each well was measured on a Molecular Devices SpectraMax Paradigm spectrophotometer.

Biodistribution studies

Tumor-bearing mice were obtained by subcutaneous injection of F9 teratocarcinoma cells (10^6) (129Sv mice) or C1498 AML cells (2×10^6; C57BL/6J mice) in the flank of 15- to 18-week-old female mice. Five days after tumor implantation, 10 μg (0.09 nmol) ^{125}I radiolabeled F8–IL2–SS–DM1 and F8–IL2 were injected into the lateral tail vein of the animals. Immunoreactivity of the antibody preparation after radioiodination was confirmed by binding to EDA resin. Mice were sacrificed 24 hours after injection. Organs were weighed, and radioactivity was counted using a Packard Cobra gamma counter, without prior perfusion. Radioactivity content of representative organs was expressed as the percentage of the injected dose per gram of tissue (%ID/g ± SE).

Therapy experiments

F9 teratocarcinoma cells (10^6; 129Sv mice) or C1498 AML cells (2×10^6; C57BL/6J mice) were injected subcutaneously into the flank of 15- to 18-week-old female mice. Five days after tumor implantation, when tumors were clearly palpable, mice were randomized in different treatment groups. Therapy was carried out by intravenous injection into the tail vein. 129Sv mice were injected 4 times, every 48 hours with 50 μg protein or saline (PBS), C57BL/6 mice were injected 3 times, every 48 hours with 10 or 30 μg protein or saline. Endpoint criteria for the experiments were a tumor size of 2,000 cm^3 or observed weight loss of more than 15% (toxicity threshold). Mice that had been rendered tumor-free for at least 40 days were considered cured. Experiments were carried out under a project license granted by the Veterinaeramt des Kantons Zuerich.

Unit conversion

The conversion of MTD values was done using the following formula Body surface (m^2)= $\sqrt{\frac{\text{height(cm)} \times \text{weight(kg)}}{3{,}600}}$ and under the assumption that the average patient has a weight of 80 kg and a height of 180 cm.

Results

Choice of DM1 as a cytotoxic payload for drug conjugates

We assessed the *in vitro* cytotoxic potential of 2 potent microtubular inhibitors (cemadotin and DM1), equipped with a thiol group suitable for protein coupling or with a methylthioether moiety (Fig. 1A). Both cemadotin and DM1 derivatives have previously been used for the

(*Continued*.) B, mean weight change is given in percentage of weight at the start of therapy for each treatment group. Mice were weighed every day. C, mean tumor volume ± SD (mm^3) is shown over time in C57BL/6 mice ($n = 5$ per treatment group) implanted s.c. with C1498 tumors. Mice were injected i.v. in the tail vein with 30 μg respectively of conjugate, immunocytokine, or saline every 48 hours for 3 injections in total (arrows). D, mean weight change is given in percentage of weight at the start of therapy for each treatment group. Mice were weighed every day. E, mean tumor volume ± SD (mm^3) is shown over time in 129Sv mice ($n = 3$ per treatment group) implanted s.c. with F9 tumors. Mice were injected i.v. in the tail vein with 30 μg respectively of conjugate, immunocytokine, or saline every 48 hours for 4 injections in total (arrows). F, mean weight change is given in percentage of weight at the start of therapy for each treatment group. Mice were weighed every day. G, mean tumor volume ± SD (mm^3) is shown over time in 129Sv mice ($n = 5$ per treatment group) implanted s.c. with F9 tumors. Mice were injected i.v. in the tail vein with 50 μg respectively of conjugate, immunocytokine, or saline every 48 hours for 4 injections in total (arrows). H, mean weight change is given in percentage of weight at the start of therapy for each treatment group. Mice were weighed every day.

Published OnlineFirst September 9, 2014; DOI: 10.1158/1535-7163.MCT-14-0599

preparation and *in* vivo testing of ADCs, based on the F8 antibody (43, 45, 46). Four murine cancer cell lines were used in the assay (F9, A20, C1498, and K1735), which we have previously shown to reproducibly grow solid tumors in immunocompetent recipient mice (36, 42, 47). Those tumors contained blood vessels, which strongly stained for EDA expression using the F8 antibody (Supplementary Fig. S1). In the cell lines, DM1 derivatives consistently exhibited a more potent cytotoxic activity than cemadotin derivatives (Fig. 1B). In line with previous reports (19), S-protected thiol drugs led to an increased anticancer activity, but DM1-SH exhibited an acceptable cytotoxic potential and was chosen as payload for the preparation of drug conjugates.

Preparation and *in vitro* characterization of chemically defined IDCs

The F8–IL2 immunocytokine was chosen as the therapeutic protein for drug coupling experiments as it had previously been shown to selectively localize to tumor blood vessels *in vivo* and to display a potent anticancer activity in immunocompetent mouse models of the disease (2, 8, 36, 42). We used the F8 antibody in scFv format (48) with a 5-aminoacid linker between VH and VL domains, driving the formation of a noncovalent homodimeric "diabody" structure (ref. 49; Supplementary Fig. S2). The antibody was genetically fused to recombinant human IL2, using a polypeptide linker with a cysteine residue (F8–IL2–SH), suitable for subsequent chemical modification strategies, or with no cysteine residue (F8–IL2; Fig. 2A). Both proteins could be expressed in mammalian cells and purified to homogeneity. In nonreducing conditions, F8–IL2–SH exhibited the formation of a disulfide-linked homodimeric product, which could however be quantitatively reduced (Fig. 2B). In addition, a variant of the F8 diabody (termed F8–SH), lacking the IL2 payload but featuring an N-terminal free cysteine residue, was expressed and purified from CHO cells. F8–IL2–SH and F8–SH were site specifically conjugated to DM1-SH using a chemical procedure based on Ellman's reagent, previously described by our group (ref. 45; Fig. 2C). All products, which were characterized by SDS-PAGE, gel filtration, and mass spectrometric analysis, were shown to be pure and homogenous (Fig. 2D).

The ability of the F8–IL2 fusion protein and of the corresponding F8–IL2–SS–DM1 drug conjugate to recognized the cognate antigen was confirmed by ELISA (not shown) and by BIAcore analysis, revealing comparable EDA-binding profiles (Fig. 3A). In addition, the IL2 moiety displayed comparable biologic activity in commercially available recombinant IL2 (Proleukin, Aldesleukin), in F8–IL2 and in F8–IL2–SS–DM1 (Fig. 3B).

In vivo tumor-targeting activity and anticancer properties of IDCs

We tested the ability of F8–IL2–SS–DM1 to preferentially accumulate in solid tumors, following intravenous administration, in mice bearing subcutaneously grafted F9 or C1498 tumors, using radioiodinated protein preparations. Twenty-four hours after intravenous administration, both F8–IL2 and F8–IL2–SS–DM1 exhibited comparable biodistribution profiles, with a preferential product accumulation in the tumor (Fig. 4). Some accumulation of the products was also observed in the kidney, in line for what had previously been reported for F8–IL2 in C1498 tumors (36) and with the renal clearance mechanism. The same tumor models were used for the study of anticancer therapeutic activity.

Immunocompetent mice bearing C1498 AML chloromas were treated with 3 injections of 10 μg of F8–IL2, F8–SS–DM1, or a combination of the 2 agents. In addition, one group of mice was treated with 10 μg doses of the F8–IL2–SS–DM1 IDC product, whereas a control group received injections of saline solution. At these doses, F8–SS–DM1 exhibited only a modest antitumor activity, whereas F8–IL2 potently inhibited tumor growth. The therapeutic action of this cytokine could be potentiated either by combination with F8–SS–DM1 or by incorporating both the IL2 and the DM1 moiety in the same product (F8–IL2–SS–DM1; Fig. 5A). None of the study groups exhibited a body weight loss greater than 5% (Fig. 5B). The experiment was repeated at higher doses (30 μg), confirming a strong anticancer activity of F8–IL2–SS–DM1 (Fig. 5C and D).

Therapeutic results obtained at 10 and 30 μg doses were similar. It is difficult to directly compare therapeutic data obtained in different sets of mice and different dates, as tumor growth rate and vascularity can slightly change across experiments.

Similar experiments were performed in Sv129Ev mice bearing subcutaneously grafted murine F9 teratocarcinomas at low (30 μg) and high (50 μg) doses, which revealed a potent antitumor activity of the IDC product, whereas none of the study groups exhibited a body weight loss greater than 10% (Fig. 5E–H).

Discussion

We have produced and characterized a novel class of armed antibody products (IDC), which combine a tumor-targeting antibody moiety and 2 therapeutic payloads in a single molecular entity. We implemented the new methodology by installing the immunostimulatory cytokine IL2 and the potent cytotoxic maytansinoid DM1 onto the clinical-stage F8 antibody. The resulting trifunctional biopharmaceutical exhibited a potent antitumor activity in 2 syngeneic murine models of cancer. Importantly, all functional moieties of the IDC retained their biologic activity and the product was able to selectively localize to tumors *in vivo*.

In the syngeneic C1498 mouse model of AML chloromas, a potent therapeutic activity could be observed at very low doses of F8–IL2–SS–DM1 (0.5 mg/kg), including some mice which were cured (Supplementary Fig. S3). This observation is encouraging, as the IDC product

Published OnlineFirst September 9, 2014; DOI: 10.1158/1535-7163.MCT-14-0599

appears to be active at substantially lower doses, compared with the ones used for the corresponding F8–SS–DM1 ADC products (43). Cost of goods may limit the industrial development of certain ADC products, and their conversion into IDC format may represent a valuable avenue for the improvement of anticancer activity. Importantly, the antibody-mediated delivery of IL2 is potently active not only in mouse models of AML but also in patients (36).

The molecular and cellular mechanisms for the observed synergy are still unknown, but we speculate that the cytotoxic damage, induced by DM1, may contribute to an increased tumor immunogenicity and vascular permeability as recently reported in other studies (2).

IDCs represent one class of multispecific antibody-based therapeutic agents. The combination of 2 binding specificities in the same antibody molecule has long attracted the interest of immunologists. BiTEs (bispecific T-cell engagers) and DART (dual-affinity retargeting platform) are representative examples of bispecific antibody products in clinical development (50, 51). Alternatively, the implementation of 2 cytokine payloads (1) or of 2 cytotoxic agents onto the same antibody molecule has also been proposed.

In principle, the IDC strategy should be broadly applicable to a variety of antibodies, cytokines, and cytotoxic agents. In practice, however, it will be important to combine payloads of comparable activity into the same IDC product, to exploit the optimal potential of this technology. The MTD of cytokines in patients may vary substantially [e.g., 9.4–132 μg/kg/d for IL2 (52), 1 μg/kg/d for IL12 (53, 54), 4 μg/kg/d for TNF (55–57), 0.5 μg/kg/d for granulocyte macrophage colony-stimulating factor (GM-CSF) (58), 0.46–0.95 μg/kg/d for IFNα (58, 59), 1–20 μg/kg/d for IL10 (60), 178 μg/kg/d for IFNβ (61)]. Similarly, the cytotoxic agents which have been used for ADC development range from doxorubicin and methotrexate, with *in vitro* cell killing potency in the 0.1 to 1 μmol/L range (62) to pyrrolobenzodiazepines which are able to kill tumor cells *in vitro* at subpicomolar concentrations (63). Should the cytokine payload be more active compared with the cytotoxic agent, it would be conceivable to fine-tune the corresponding biologic activity by amino acid mutations. Indeed, there is growing evidence that certain cytokine mutants (e.g., the IL2 "superkine"-bearing mutations in 5 amino acid residues) may acquire beneficial properties, such as improved proliferation induction potential of T cells irrespective of the presence of the normally essential high-affinity α-subunit of IL2 receptor, more potent induction of downstream phosphorylation signal improved *in vivo* antitumor activity, and reduced expansion of regulatory T cells (Treg; ref. 64).

The combined use of immunostimulatory cytokines and cytotoxic compounds may be counterintuitive, as the anticancer drug could kill leukocytes *in vivo* and therefore inhibit cytokine activity. However, there is growing evidence that the mechanism of action of anticancer cytotoxic drugs may be more complex. For example, certain chemotherapeutic agents have been shown to significantly potentiate the antitumor effect of immunocytokines. Specifically, inefficient extravasation of drug and immune cells toward to site of disease is a major obstacle for efficacious targeted therapy, which can be overcome by pretreatment with chemotherapeutic agents. Paclitaxel increases vascular permeability in tumors (2) and reduces interstitial fluid pressure (16, 17). These mechanisms lead to enhanced infiltration and activation of leukocytes (2, 18) and provide a rationale for the combined use of cytotoxic small-molecule drugs and cytokines.

Cytotoxic drugs may exert immunostimulatory effects by influencing the functions of effector cells of the immune system, by lymphodepletion, or subversion of immunosuppressive mechanisms (5). For example, gemcitabine-induced apoptosis in established tumors enhances dendritic cell–dependent cross-presentation of tumor antigens (65, 66), increasing the sensitivity of tumor cells to lytic killing by cytotoxic T cells (67, 68). Both gemcitabine and cyclophosphamide have been shown to reduce the number and inhibitory function of Tregs (69–71).

In practice, the identification of the recommended dose for pharmacologic treatment will require the study of activity and tolerability at multiple dose levels. In the field of cancer immunotherapy, the implementation of larger phase I clinical trials, with a sufficient number of patients in each cohort for the determination of therapeutic activity, is becoming more and more common. For instance, 2 recent examples of remarkable results in clinical melanoma treatment obtained with the use of anti-PD-1 antibodies (lambrolizumab from Merck and nivolumab by Bristol-Meyer-Squibb) relied on large cohorts of patients at each dose level, in phase I studies (72, 73).

It is well-established that the pharmacotherapy of cancer relies, in most cases, on combination therapy. The development of multifunctional products, such as the IDCs described in this article, should avoid the parallel clinical development of individual agents, which may lack sufficient activity when used as monotherapy. The traditional "one-at-a-time" development of anticancer drugs is not only costly and time-consuming but may also deny patients the option of a potentially efficacious treatment. In particular, the chemically defined incorporation of an IL2 moiety and of a potent cytotoxic agent into a single biopharmaceutical agent holds promises for the therapy of AML, as ADCs and IL2-based immunocytokines have already exhibited promising activity both in animal models and in patients with cancer (6, 7, 14, 15, 21, 41, 74–77)

Disclosure of Potential Conflicts of Interest

D. Neri has ownership interest (including patents) in and is a consultant/advisory board member for Philogen. No potential conflicts of interest were disclosed by the other authors.

Authors' Contributions

Conception and design: T. List, G. Casi, D. Neri

Published OnlineFirst September 9, 2014; DOI: 10.1158/1535-7163.MCT-14-0599

Development of methodology: T. List, G. Casi, D. Neri
Acquisition of data (provided animals, acquired and managed patients, provided facilities, etc.): T. List
Analysis and interpretation of data (e.g., statistical analysis, biostatistics, computational analysis): T. List, D. Neri
Writing, review, and/or revision of the manuscript: T. List, D. Neri
Administrative, technical, or material support (i.e., reporting or organizing data, constructing databases): T. List
Study supervision: D. Neri

Acknowledgments

The authors thank Sabrina Trüssel for providing the F8–SH diabody intermediate, as well as Elena Perrino and Nikolaus Krall for DM1 and Cem derivatives for *in vitro* studies.

Grant Support

Financial support was provided to D. Neri from ETH Zurich, the Maiores Foundation, the Federal Commission for Technology and Innovation (CTI; grants ADC and Medtech #12803.1), Swiss-Japanese Research Collaboration, and the Swiss National Science Foundation (#310030_144091).

The costs of publication of this article were defrayed in part by the payment of page charges. This article must therefore be hereby marked *advertisement* in accordance with 18 U.S.C. Section 1734 solely to indicate this fact.

Received July 23, 2014; revised August 27, 2014; accepted August 29, 2014; published OnlineFirst September 9, 2014.

References

1. Halin C, Gafner V, Villani ME, Borsi L, Berndt A, Kosmehl H, et al. Synergistic therapeutic effects of a tumor targeting antibody fragment, fused to interleukin 12 and to tumor necrosis factor alpha. Cancer Res 2003;63:3202–10.
2. Moschetta M, Pretto F, Berndt A, Galler K, Richter P, Bassi A, et al. Paclitaxel enhances therapeutic efficacy of the F8-IL2 immunocytokine to EDA-fibronectin-positive metastatic human melanoma xenografts. Cancer Res 2012;72:1814–24.
3. List T, Neri D. Immunocytokines: a review of molecules in clinical development for cancer therapy. Clin Pharmacol 2013;5:29–45.
4. Kreuser ED, Wadler S, Thiel E. Biochemical modulation of cytotoxic drugs by cytokines: molecular mechanisms in experimental oncology. Recent Results Cancer Res 1995;139:371–82.
5. Baxevanis CN, Perez SA, Papamichail M. Combinatorial treatments including vaccines, chemotherapy and monoclonal antibodies for cancer therapy. Cancer Immunol Immunother 2009;58: 317–24.
6. Marlind J, Kaspar M, Trachsel E, Sommavilla R, Hindle S, Bacci C, et al. Antibody-mediated delivery of interleukin-2 to the stroma of breast cancer strongly enhances the potency of chemotherapy. Clin Cancer Res 2008;14:6515–24.
7. Pedretti M, Verpelli C, Marlind J, Bertani G, Sala C, Neri D, et al. Combination of temozolomide with immunocytokine F16-IL2 for the treatment of glioblastoma. Br J Cancer 2010;103:827–36.
8. Frey K, Schliemann C, Schwager K, Giavazzi R, Johannsen M, Neri D. The immunocytokine F8-IL2 improves the therapeutic performance of sunitinib in a mouse model of renal cell carcinoma. J Urol 2010; 184:2540–8.
9. Eigentler TK, Weide B, de Braud F, Spitaleri G, Romanini A, Pflugfelder A, et al. A dose-escalation and signal-generating study of the immunocytokine L19-IL2 in combination with dacarbazine for the therapy of patients with metastatic melanoma. Clin Cancer Res 2011;17: 7732–42.
10. Hess C, Venetz D, Neri D. Emerging classes of armed antibody therapeutics against cancer. Medchemcomm 2014;5:408–31.
11. Wagner K, Schulz P, Scholz A, Wiedenmann B, Menrad A. The targeted immunocytokine L19-IL2 efficiently inhibits the growth of orthotopic pancreatic cancer. Clin Cancer Res 2008;14:4951–60.
12. Papadia F, Basso V, Patuzzo R, Maurichi A, Di Florio A, Zardi L, et al. Isolated limb perfusion with the tumor-targeting human monoclonal antibody-cytokine fusion protein L19-TNF plus melphalan and mild hyperthermia in patients with locally advanced extremity melanoma. J Surg Oncol 2013;107:173–9.
13. Gillies SD. Immunocytokines: a novel approach to cancer immune therapy. Targeted Cancer Immune Ther 2009: 241–56
14. De Braud F, Catania C, Masini C, Maur M, Cascinu S, Berardi R, et al. Combinations of the immunocytokine F16-IL2 with doxorubicin or with paclitaxel investigated in phase Ib studies in patients with advanced solid tumors. J Clin Oncol 28, 2010 (suppl; abstr e13017).
15. De Braud F, Catania C, Onofri A, Pierantoni C, Cascinu S, Maur M, et al. Combination of the immunocytokine F16-IL2 with doxorubicin or paclitaxel in patients with solid tumors: results from two phase Ib trials. J Clin Oncol 29, 2011 (suppl; abstr 2595).
16. Griffon-Etienne G, Boucher Y, Brekken C, Suit HD, Jain RK. Taxane-induced apoptosis decompresses blood vessels and lowers interstitial fluid pressure in solid tumors: clinical implications. Cancer Res 1999;59:3776–82.
17. Bronstad A, Berg A, Reed RK. Effects of the taxanes paclitaxel and docetaxel on edema formation and interstitial fluid pressure. Am J Physiol Heart Circ Physiol 2004;287:H963–8.
18. Mason K, Staab A, Hunter N, McBride W, Petersen S, Terry N, et al. Enhancement of tumor radioresponse by docetaxel: involvement of immune system. Int J Oncol 2001;18:599–606.
19. Chari RV, Miller ML, Widdison WC. Antibody-drug conjugates: an emerging concept in cancer therapy. Angew Chem Int Ed Engl 2014;53:3796–827.
20. Wu AM, Senter PD. Arming antibodies: prospects and challenges for immunoconjugates. Nat Biotechnol 2005;23:1137–46.
21. Schwager K, Hemmerle T, Aebischer D, Neri D. The immunocytokine L19-IL2 eradicates cancer when used in combination with CTLA-4 blockade or with L19-TNF. J Invest Dermatol 2013; 133:751–8.
22. Bumol TF, Wang QC, Reisfeld RA, Kaplan NO. Monoclonal antibody and an antibody-toxin conjugate to a cell surface proteoglycan of melanoma cells suppress *in vivo* tumor growth. Proc Natl Acad Sci U S A 1983;80:529–33.
23. Schrappe M, Bumol TF, Apelgren LD, Briggs SL, Koppel GA, Markowitz DD, et al. Long-term growth suppression of human glioma xenografts by chemoimmunoconjugates of 4-desacetylvinblastine-3-carboxyhydrazide and monoclonal antibody 9.2.27. Cancer Res 1992; 52:3838–44.
24. Sivam GP, Martin PJ, Reisfeld RA, Mueller BM. Therapeutic efficacy of a doxorubicin immunoconjugate in a preclinical model of spontaneous metastatic human melanoma. Cancer Res 1995;55:2352–6.
25. Helguera G, Morrison SL, Penichet ML. Antibody-cytokine fusion proteins: harnessing the combined power of cytokines and antibodies for cancer therapy. Clin Immunol 2002;105:233–46.
26. Weide B. Tumor-targeting human L19IL2 monoclonal antibody-cytokine fusion protein in combination with DTIC in chemotherapy-naïve stage IV melanoma patients. J Clin Oncol 28:15s, 2010 (suppl; abstr 8555).
27. Gutbrodt KL, Casi G, Neri D. Antibody-based delivery of IL2 and cytotoxics eradicates tumors in immunocompetent mice. Mol Cancer Ther 2014;13:1772–6.
28. Pasche N, Wulhfard S, Pretto F, Carugati E, Neri D. The antibody-based delivery of interleukin-12 to the tumor neovasculature eradicates murine models of cancer in combination with paclitaxel. Clin Cancer Res 2012;18:4092–103.
29. Frey K, Zivanovic A, Schwager K, Neri D. Antibody-based targeting of interferon-alpha to the tumor neovasculature: a critical evaluation. Integr Biol (Camb) 2011;3:468–78.
30. Brack SS, Silacci M, Birchler M, Neri D. Tumor-targeting properties of novel antibodies specific to the large isoform of tenascin-C. Clin Cancer Res 2006;12:3200–8.
31. Borsi L, Balza E, Bestagno M, Castellani P, Carnemolla B, Biro A, et al. Selective targeting of tumoral vasculature: comparison of different

Published OnlineFirst September 9, 2014; DOI: 10.1158/1535-7163.MCT-14-0599

formats of an antibody (L19) to the ED-B domain of fibronectin. Int J Cancer 2002;102:75–85.
32. Demartis S, Tarli L, Borsi L, Zardi L, Neri D. Selective targeting of tumour neovasculature by a radiohalogenated human antibody fragment specific for the ED-B domain of fibronectin. Eur J Nucl Med 2001;28:534–9.
33. Schwager K, Kaspar M, Bootz F, Marcolongo R, Paresce E, Neri D, et al. Preclinical characterization of DEKAVIL (F8-IL10), a novel clinical-stage immunocytokine which inhibits the progression of collagen-induced arthritis. Arthritis Res Ther 2009;11:R142.
34. Berndt A, Koellner R, Richter P, Franz M, Voigt A, Berndt A, et al. A comparative analysis of oncofetal fibronectin and tenascin-C incorporation in tumour vessels using human recombinant SIP format antibodies. Histochem Cell Biol 2010;133:467–75.
35. Schliemann C, Wiedmer A, Pedretti M, Szczepanowski M, Klapper W, Neri D. Three clinical-stage tumor targeting antibodies reveal differential expression of oncofetal fibronectin and tenascin-C isoforms in human lymphoma. Leuk Res 2009;33:1718–22.
36. Gutbrodt KL, Schliemann C, Giovannoni L, Frey K, Pabst T, Klapper W, et al. Antibody-based delivery of interleukin-2 to neovasculature has potent activity against acute myeloid leukemia. Sci Transl Med 2013;5:201ra118.
37. Villa A, Trachsel E, Kaspar M, Schliemann C, Sommavilla R, Rybak JN, et al. A high-affinity human monoclonal antibody specific to the alternatively spliced EDA domain of fibronectin efficiently targets tumor neo-vasculature *in vivo*. Int J Cancer 2008;122:2405–13.
38. McDermott DF, Regan MM, Atkins MB. Interleukin-2 therapy of metastatic renal cell carcinoma: update of phase III trials. Clin Genitourin Cancer 2006;5:114–9.
39. McDermott DF, Regan MM, Clark JI, Flaherty LE, Weiss GR, Logan TF, et al. Randomized phase III trial of high-dose interleukin-2 versus subcutaneous interleukin-2 and interferon in patients with metastatic renal cell carcinoma. J Clin Oncol 2005;23:133–41.
40. Philip PA. Interleukin-2 in the treatment of malignant melanoma. Expert Opin Investig Drugs 1998;7:361–71.
41. Johannsen M, Spitaleri G, Curigliano G, Roigas J, Weikert S, Kempkensteffen C, et al. The tumour-targeting human L19-IL2 immunocytokine: preclinical safety studies, phase I clinical trial in patients with solid tumours and expansion into patients with advanced renal cell carcinoma. Eur J Cancer 2010;46:2926–35.
42. Hemmerle T, Neri D. The antibody-based targeted delivery of interleukin-4 and 12 to the tumor neovasculature eradicates tumors in three mouse models of cancer. Int J Cancer 2014;134:467–77.
43. Perrino E, Steiner M, Krall N, Bernardes GJ, Pretto F, Casi G, et al. Curative properties of noninternalizing antibody-drug conjugates based on maytansinoids. Cancer Res 2014;74:2569–78.
44. Rajendra Y, Kiseljak D, Baldi L, Hacker DL, Wurm FM. A simple high-yielding process for transient gene expression in CHO cells. J Biotechnol 2011;153:22–6.
45. Bernardes GJ, Casi G, Trussel S, Hartmann I, Schwager K, Scheuermann J, et al. A traceless vascular-targeting antibody-drug conjugate for cancer therapy. Angew Chem Int Ed Engl 2012;51:941–4.
46. Casi G, Huguenin-Dezot N, Zuberbuhler K, Scheuermann J, Neri D. Site-specific traceless coupling of potent cytotoxic drugs to recombinant antibodies for pharmacodelivery. J Am Chem Soc 2012;134:5887–92.
47. Pretto F, Elia G, Castioni N, Neri D. Preclinical evaluation of IL2-based immunocytokines supports their use in combination with dacarbazine, paclitaxel and TNF-based immunotherapy. Cancer Immunol Immunother 2014;63:901–10.
48. Huston JS, Levinson D, Mudgett-Hunter M, Tai MS, Novotny J, Margolies MN, et al. Protein engineering of antibody binding sites: recovery of specific activity in an anti-digoxin single-chain Fv analogue produced in *Escherichia coli*. Proc Natl Acad Sci U S A 1988;85:5879–83.
49. Holliger P, Hudson PJ. Engineered antibody fragments and the rise of single domains. Nat Biotechnol 2005;23:1126–36.
50. Moore PA, Zhang W, Rainey GJ, Burke S, Li H, Huang L, et al. Application of dual affinity retargeting molecules to achieve optimal redirected T-cell killing of B-cell lymphoma. Blood 2011;117:4542–51.
51. Bargou R, Leo E, Zugmaier G, Klinger M, Goebeler M, Knop S, et al. Tumor regression in cancer patients by very low doses of a T cell-engaging antibody. Science 2008;321:974–7.
52. Yang JC, Sherry RM, Steinberg SM, Topalian SL, Schwartzentruber DJ, Hwu P, et al. Randomized study of high-dose and low-dose interleukin-2 in patients with metastatic renal cancer. J Clin Oncol 2003;21:3127–32.
53. Atkins MB, Robertson MJ, Gordon M, Lotze MT, DeCoste M, DuBois JS, et al. Phase I evaluation of intravenous recombinant human interleukin 12 in patients with advanced malignancies. Clin Cancer Res 1997;3:409–17.
54. Gollob JA, Mier JW, Veenstra K, McDermott DF, Clancy D, Clancy M, et al. Phase I trial of twice-weekly intravenous interleukin 12 in patients with metastatic renal cell cancer or malignant melanoma: ability to maintain IFN-gamma induction is associated with clinical response. Clin Cancer Res 2000;6:1678–92.
55. Gamm H, Lindemann A, Mertelsmann R, Herrmann F. Phase I trial of recombinant human tumour necrosis factor alpha in patients with advanced malignancy. Eur J Cancer 1991;27:856–63.
56. Bonvalot S, Laplanche A, Lejeune F, Stoeckle E, LePechoux C, Vanel D, et al. Limb salvage with isolated perfusion for soft tissue sarcoma: could less TNF-alpha be better? Ann Oncol 2005;16:1061–8.
57. Eggermont AM, Schraffordt Koops H, Klausner JM, Kroon BB, Schlag PM, Lienard D, et al. Isolated limb perfusion with tumor necrosis factor and melphalan for limb salvage in 186 patients with locally advanced soft tissue extremity sarcomas. The cumulative multicenter European experience. Ann Surg 1996;224:756–64; discussion 764–5.
58. Garcia JA, Mekhail T, Elson P, Wood L, Bukowski RM, Dreicer R, et al. Phase I/II trial of subcutaneous interleukin-2, granulocyte-macrophage colony-stimulating factor and interferon-alpha in patients with metastatic renal cell carcinoma. BJU Int 2012;109:63–9.
59. Garbe C, Peris K, Hauschild A, Saiag P, Middleton M, Spatz A, et al. Diagnosis and treatment of melanoma: European consensus-based interdisciplinary guideline. Eur J Cancer 2010;46:270–83.
60. Fedorak RN, Gangl A, Elson CO, Rutgeerts P, Schreiber S, Wild G, et al. Recombinant human interleukin 10 in the treatment of patients with mild to moderately active Crohn's disease. The Interleukin 10 Inflammatory Bowel Disease Cooperative Study Group. Gastroenterology 2000;119:1473–82.
61. Ravandi F, Estrov Z, Kurzrock R, Breitmeyer JB, Maschek BJ, Talpaz M. A phase I study of recombinant interferon-beta in patients with advanced malignant disease. Clin Cancer Res 1999;5:3990–8.
62. Krall N, Scheuermann J, Neri D. Small targeted cytotoxics: current state and promises from DNA-encoded chemical libraries. Angew Chem Int Ed Engl 2013;52:1384–402.
63. Hartley JA, Hamaguchi A, Coffils M, Martin CR, Suggitt M, Chen Z, et al. SG2285, a novel C2-aryl-substituted pyrrolobenzodiazepine dimer prodrug that cross-links DNA and exerts highly potent antitumor activity. Cancer Res 2010;70:6849–58.
64. Levin AM, Bates DL, Ring AM, Krieg C, Lin JT, Su L, et al. Exploiting a natural conformational switch to engineer an interleukin-2 'superkine'. Nature 2012;484:529–33.
65. Nowak AK, Lake RA, Marzo AL, Scott B, Heath WR, Collins EJ, et al. Induction of tumor cell apoptosis *in vivo* increases tumor antigen cross-presentation, cross-priming rather than cross-tolerizing host tumor-specific CD8 T cells. J Immunol 2003;170:4905–13.
66. Nowak AK, Robinson BW, Lake RA. Synergy between chemotherapy and immunotherapy in the treatment of established murine solid tumors. Cancer Res 2003;63:4490–6.
67. Tanaka F, Yamaguchi H, Ohta M, Mashino K, Sonoda H, Sadanaga N, et al. Intratumoral injection of dendritic cells after treatment of anticancer drugs induces tumor-specific antitumor effect *in vivo*. Int J Cancer 2002;101:265–9.
68. Hu HM, Poehlein CH, Urba WJ, Fox BA. Development of antitumor immune responses in reconstituted lymphopenic hosts. Cancer Res 2002;62:3914–9.
69. Lutsiak ME, Semnani RT, De Pascalis R, Kashmiri SV, Schlom J, Sabzevari H. Inhibition of CD4(+)25+ T regulatory cell function

Published OnlineFirst September 9, 2014; DOI: 10.1158/1535-7163.MCT-14-0599

implicated in enhanced immune response by low-dose cyclophosphamide. Blood 2005;105:2862–8.

70. Schiavoni G, Mattei F, Di Pucchio T, Santini SM, Bracci L, Belardelli F, et al. Cyclophosphamide induces type I interferon and augments the number of CD44(hi) T lymphocytes in mice: implications for strategies of chemoimmunotherapy of cancer. Blood 2000;95:2024–30.
71. Mortara L, Orecchia P, Castellani P, Borsi L, Carnemolla B, Balza E. Schedule-dependent therapeutic efficacy of L19mTNF-alpha and melphalan combined with gemcitabine. Cancer Med 2013;2:478–87.
72. Hamid O, Robert C, Daud A, Hodi FS, Hwu WJ, Kefford R, et al. Safety and tumor responses with lambrolizumab (anti-PD-1) in melanoma. N Engl J Med 2013;369:134–44.
73. Topalian SL. Nivolumab (anti-PD-1; BMS-936558; ONO-4538) in patients with advanced solid tumors: survival and long-term safety in a phase I trial. 2013 ASCO annual meeting; 2013: J Clin Oncol 31, 2013 (suppl; abstr 3002).
74. Lode HN, Xiang R, Varki NM, Dolman CS, Gillies SD, Reisfeld RA. Targeted interleukin-2 therapy for spontaneous neuroblastoma metastases to bone marrow. J Natl Cancer Inst 1997;89:1586–94.
75. Lode HN, Xiang R, Dreier T, Varki NM, Gillies SD, Reisfeld RA. Natural killer cell-mediated eradication of neuroblastoma metastases to bone marrow by targeted interleukin-2 therapy. Blood 1998;91:1706–15.
76. Yamane BH, Hank JA, Albertini MR, Sondel PM. The development of antibody-IL-2 based immunotherapy with hu14.18-IL2 (EMD-273063) in melanoma and neuroblastoma. Expert Opin Investig Drugs 2009;18:991–1000.
77. Laurent J, Touvrey C, Gillessen S, Joffraud M, Vicari M, Bertrand C, et al. T-cell activation by treatment of cancer patients with EMD 521873 (Selectikine), an IL-2/anti-DNA fusion protein. J Transl Med 2013;11:5.

Published OnlineFirst September 9, 2014; DOI: 10.1158/1535-7163.MCT-14-0599

Molecular Cancer Therapeutics

A Chemically Defined Trifunctional Antibody–Cytokine–Drug Conjugate with Potent Antitumor Activity

Thomas List, Giulio Casi and Dario Neri

Mol Cancer Ther 2014;13:2641-2652. Published OnlineFirst September 9, 2014.